

Stability analysis of support systems using a coupled FEM-DFN model (Case study: a diversion tunnel at Lorestan dam site, Iran)

M. Noroozi^{1*}, R. Rafiee¹ and M. Najafi²

1. Faculty of Mining, Petroleum & Geophysics Engineering, Shahrood University of Technology, Shahrood, Iran
2. Department of Mining and Metallurgical Engineering, Yazd University, Yazd, Iran

Received 28 July 2017; received in revised form 1 December 2017; accepted 14 February 2018

*Corresponding author: mehdi.noroozi@shahroodut.ac.ir (M. Noroozi).

Abstract

Various structural discontinuities, which form a discrete fracture network, play a significant role in the failure conditions and stability of the rock masses around underground excavations. Several continuum numerical methods have been used to study the stability of underground excavations in jointed rock masses but only few of them can take into account the influence of the pre-existing natural fractures. In this work, the pre-existing fractures are explicitly modeled as a Discrete Fracture Network (DFN) model, which is fully coupled with the FEM modeling for stability analysis of support systems in a diversion tunnel at the Rudbar Lorestan dam site. Hence, at first, using the surveyed data in the diversion tunnel and an estimation of the suitable probability distribution function on geometric characteristics of the existing joint sets in this region, the 3D DFN model was simulated using the stochastic discrete fracture networks generator program, DFN-FRAC^{3D}. In the second step, a coupled 2D Finite Element Method and the prepared stochastic model were used for analysis of existent (based on technical reports) recommended support systems. The objective here is to grasp the role of the fracture networks on the results of the tunnel stability analysis using FEM modeling and also to compare the results with those obtained through stability analysis without considering the effect of fractures.

Keywords: Tunnel Stability Analysis, Finite Element Method, Discrete Fracture Network.

1. Introduction

Excavation of an underground tunnel in a discontinuous rock mass can lead to deformation and stress redistribution. Most naturally occurring discontinuous rock masses comprise intact rock interspaced with different types of discontinuities. Such discontinuities include fissures, fractures, faults, bedding planes, shear zones, and dykes. The existence and behavior of discontinuities in a rock mass will influence the mechanical behavior of the discontinuous rock mass. Rock fractures are by far the most common discontinuity encountered in rock masses [1].

The first step in the study of the mechanical behavior of underground excavations in fractured rock masses is to design a geometrical model of joint networks based on the geometrical data obtained from the earth [2]. In other words, the

main issue in rock mass modelling is to attain a precise 3D description of rock mass structures through the collected data [3]. However, there will always be some random variations in the geometric properties of fractures such as dip, dip direction, spacing, and persistence by virtue of rock mass heterogeneous nature. Therefore, it is necessary to describe the ordered properties stochastically and to use in rock mass modeling [4]. The 3D stochastic fracture network modeling technique represents the most optimal choice for simulating the probability nature of fracture geometric properties.

The next step in the study of the mechanical behavior is to analyze the stress around an underground excavation using the prepared geometrical model. In general, either the

discontinuum or the equivalent continuum stress analysis method has been used to incorporate the influence of fractures in stability or failure analysis of underground excavations in fractured rock masses [5].

Typically, in an industry project, the equivalent environment is used for modeling the jointed rock mass, and the direct impact of the joint sets is not considered. This simplification can lead to some errors. In this paper, for the first time, the 2D finite element software PHASE² Version 8.005 (that is able to model joints with a limited size) is used to assess the role of joints in the underground space stability. Also, in this work, in order to avoid any simplification, the DFN modeling is used to model the joint sets network. The modeling method presented in this paper can be considered as one of the first models of the FEM-DFN couple.

The purpose of this work was to evaluate the geotechnical behavior around the diversion tunnel in the Rudbar Lorestan dam site by considering the effect of fractures using a continuum model and the following software packages: (a) stochastic fracture networks generator code DFN-FRAC^{3D} [6, 7] that forms finite size fractures in 3-D with geometrical features that are described stochastically. Using this code and the surveyed data in the diversion tunnel, the 3D geometrical-stochastic model of fracture networks (3D-DFN model) was prepared; and (b) commercial software based on the finite element method, PHASE².

2. Literature review

The important steps involved in rock mass analysis are to present a precise definition of the discontinuities network (creating a geometrical model) and to evaluate its stability.

Stochastic models of fracture networks show the heterogeneous nature of the fractured rock masses, considering the fracture network as discrete elements in space with geometrical features that are described stochastically [8]. The geologic stochastic models developed at MIT can be considered as the initial models prepared in this field. Its wider application to rock engineering was promoted in the 1980s by the works of several research groups [2, 9-11]. Further research works were carried out on basic fracturing processes to develop a hierarchical fracture geometry model and to simulate fluid flow and slope stability analysis [12-16]. In the recent years, the 2D and 3D stochastic models have been developed to examine the effects of considering or

not considering the correlation between distributions of fracture apertures and fracture trace lengths on the hydro-mechanical behavior of fractured rocks [17-19].

On the other hand, several numerical methods have been used to perform stress analyses and to evaluate stability of underground excavations in fractured rock masses by incorporating discontinuities. Yoshida and Horii [20] have developed a micromechanics-based continuum model of a fractured rock mass and applied it using the finite element method to analyze the stability of underground excavations. Sitharam et al. [21] and Sitharam and Latha [22] have represented fractured rock mass as an equivalent continuum using an empirical approach and incorporating the effects of joints through a joint factor, and then have investigated the stability of caverns using the finite element method and the finite difference method, respectively. Torano et al. [23] have used the finite element method with a simplified form of discontinuities to perform stability analysis of mine roadway tunnels. Zhu et al. [24] have performed 3D finite element analysis to study the effects of rock mass parameters, rock support systems, and different excavation scenarios on tunnel stability. Basarir [25] has evaluated the performance of a proposed rock support system for a diversion tunnel in a dam site using a 2D finite element analysis. Genis et al. [26] have examined the performance of a proposed rock support system for a road way tunnel using a 2D finite element analysis. The necessary rock mass geomechanical parameters for this study have been estimated by means of rock mass classification systems. Cai [27] has studied the influence of stress path on tunnel excavation response using FLAC^{2D} and PHASE² (based on the finite element technique). Coggan et al. [28] have studied the effect of weak immediate roof lithology on coal mine roadway stability using PHASE², EXAMINE^{3D}, and FLAC^{3D}. Wu and Kulatilake [5] have studied the deformation and stability around a diversion tunnel using an equivalent continuum technique and a 3D fracture network having infinite size fractures.

Although the distinct element method that is based upon discontinuum modeling techniques are better suited than the finite element method that is based upon the continuum theory to perform discontinuum analysis of underground excavations in fractured rock masses, in many cases, in the industry, and in some cases, researchers have used the finite element software and the continuum analysis method to incorporate

the effect of fractures in underground excavation stability evaluations. The main purpose of this article was to alert for the use of such stability analysis, especially in the industry. Therefore, In order to have the models that have the closest similarities to the conventional models used in the industry, the software used in this project was also PHASE². In this way, the difference between the results of jointed models and equivalent models in the stability analyzes could be expressed more definitively and in absolute terms.

However, none of the aforementioned underground excavation applications were considered as a 3D stochastic fracture network, as the most optimal choice for simulating the probability nature of fractured rock mass in conjunction with a continuum stress analysis that is capable of incorporating the finite size fractures explicitly. In this work, the continuum approach considering the finite size fractures was performed using a 3D DFN model including finite size fractures to investigate the stability around the selected diversion tunnel and to make a comparison with the results obtained through the continuum approach without considering the fracture network.

3. Location and geology of Lorestan Rudbar dam

The project was performed in the Lorestan Rudbar dam and hydropower plant in the Lorestan province, 100 km far from the southern boundary of Aligudarz and in the way of Rudbar River

(Figure 1). The area under study was located across northern Zagros, which was limited to Zagros folded belt from SW and to Zagros main reverse fault and Sanandaj-Sirjan zone from NE. Topographically, the average height of this area was about 1750 m, and it had a cold and mountainous weather.

In the area under study, the most important exposed units were limestone-dolomite formations of the Dalan and Seruk belonging to the Permian period, Hormoz and Mila formations with shale and marl lithology belonging to Cambrian period, and Groo formation with marl-limestone and marl belonging to Cretaceous period and Bakhtiary formation, which were made up of conglomerate belonging to Pliocene period. Reverse or thrust faults, which were the main tectonic factors in the area, made the rocks appear folded. The faults had a great variety due to being located along Zagros. The overall trend of the area geological structure was from N130E to N140E called Zagros trend. Rock masses surrounding the dam site were mainly composed of carbonaceous with a specific gravity of 2.7 g/cm³. They had low porosity and also bedding. The thickness of the layers varied from thin layers to the thick ones.

From the perspective of rock quality designation (RQD), according to the exploratory drillings, rock mass did not have the desired conditions, and the average of RQD showed a mid to low quality. Furthermore, based on RMR ranking, the quality of rock mass was measured to be mid [29].

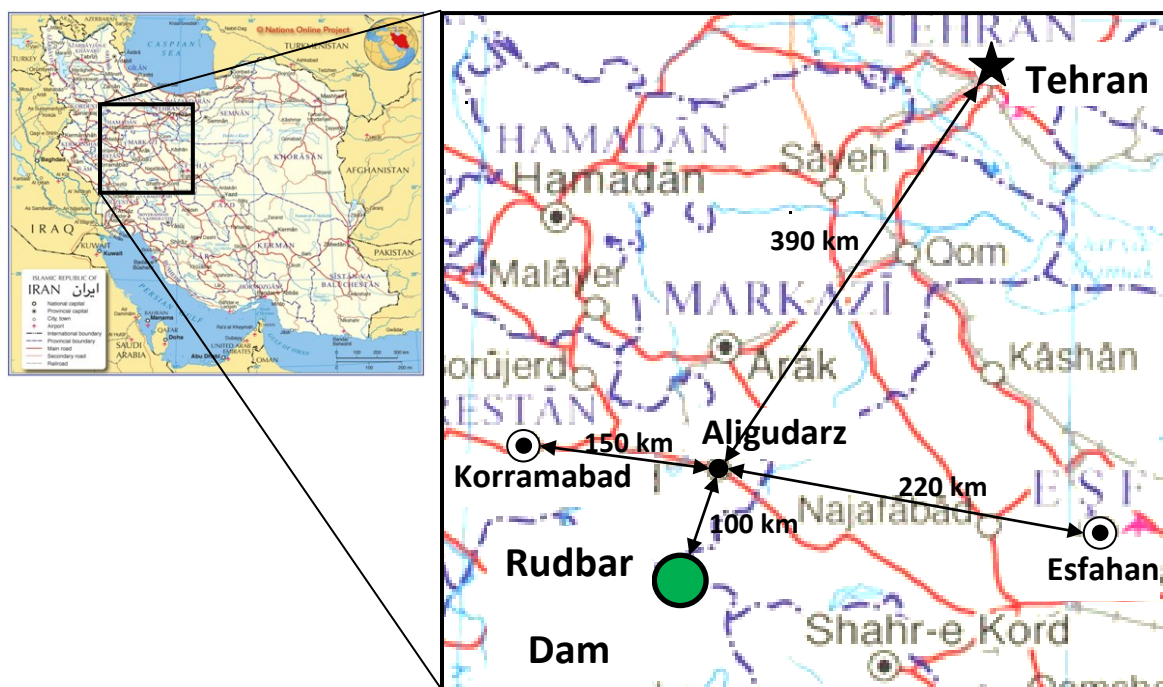


Figure 1. Location of Lorestan Roodbar dam.

4. 3D stochastic fracture networks modeling of studied area

The first step in the underground structure analysis was to design a geometrical model of rock masses. In this section, a 3D geometrical-stochastical model of fracture networks around the diversion tunnel in the dam site was prepared.

4.1. Field studies

The first stage of the geometrical modeling process is to collect discontinuity data for statistical analysis. Geometrical features of the fracture are normally determined by surveying the fractures along the rock surface through linear or window survey methods [30]. In this work, the scanline mapping technique was used. The scanline sampling technique involves measuring all the fractures that intersect a scanline along its length. In this technique, a clean, approximately planar rock face is selected that is large relative to the size and spacing of discontinuities. As a rough guide, the sample zone should contain between 150 and 350 fractures, about 50% of which should

have at least one end visible. The surveyed line has a tape length of 20 to 30 m, and is stabilized by two nails along the exposure with the steepest dip [12].

In order to have an perspective of the type of termination of the fracture trace length in the exposure, let the numbers belonging to the three types of traces be p , m , and n for joints with both ends of the trace censored, one end of trace censored, and both ends of the trace observable, respectively. Then the values for R_0 , R_1 , and R_2 are defined as follow [31]:

$$\begin{aligned} R_0 &= \frac{p}{(p+m+n)} \\ R_1 &= \frac{m}{(p+m+n)} \\ R_2 &= \frac{n}{(p+m+n)} \end{aligned} \quad (1)$$

The diversion tunnel entrance, the surveying line, and the rock exposure that are located exactly above and along the tunnel axis are shown in Figure 2. In Table 1, a summary of the surveyed fractures is presented.



Figure 2. Diversion tunnel, rock exposure, and surveying line.

Table 1. Summary of surveyed joints.

Mean trace length (m)	Termination type (%)			Number of joints	Rock type
	R ₂	R ₁	R ₀		
2.02	71	26	3	177	Dolomite-Limestone

4.2. Statistical analysis of surveyed fracture geometrical features

The appropriate data required for statistical studies can be obtained by discriminating each set and specifying its related features such as dip, dip direction, spacing, and persistence.

4.2.1. Fracture orientation distribution

Mapping of joint dips and directions were conducted in the field. Joint orientations were processed utilizing the commercially available

software DIPS 5.103 based on the equal-area stereographic projection, and the major joint sets were distinguished for dolomite-limestone (Figure 3). It has been shown that the dip direction follows a uniform distribution, and the dip angle follows the Fischer distribution [12, 32]. In this work, these distributions were used for joint orientations. Fischer constant for each joint set was obtained using the Dips software (Table 2).

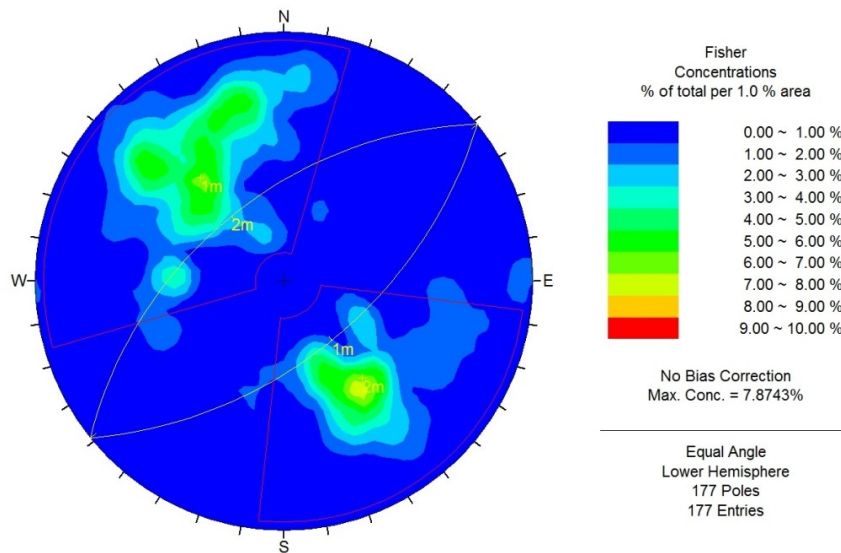


Figure 3. Separation of joint sets in Schmidt network.

Table 2. Geometrical parameters of surveyed joint sets.

Joint set orientation (Dip/DDir)	Fisher constant (K)	Intensity, P ₃₂ (m ⁻¹)	Distribution function	Length distribution parameters			
				Scale parameter (σ)	Location parameter (μ)	Mean	Standard Deviation
1 (56/141)	9.9	0.25	lognormal	σ = 0.937	μ = 0.121	2.42	2.51
2 (52/320)	16.3	0.08	Gamma	α = 0.726	β = 3.334	1.81	2.16

4.2.2. Fracture intensity

Totally, volumetric fracture intensity (square meters/cubic meters), P₃₂, is obtained from the surveyed surface fracture intensity (meter/square meters), P₂₁. Zhang and Einstein [15] have proposed the following equation to calculate P₃₂:

$$P_{32} = \frac{N_T E(A)}{V} \tag{2}$$

where N_T is the total number of sampled discontinuities, E(A) is the mean discontinuity

area, and V is the unit volume (here considered 1 m³).

Here, the number of fractures was counted by one square meter framework with ten square centimetres meshed networks (Figure 4). The fractures crossing each meshed line were counted and the total number of counted fractures in one square meter framework was defined as the surface fracture intensity [33]. Through the use of the field measurements and using Equation 2, the amounts of P₃₂ were calculated separately for each fracture set (Table 2).

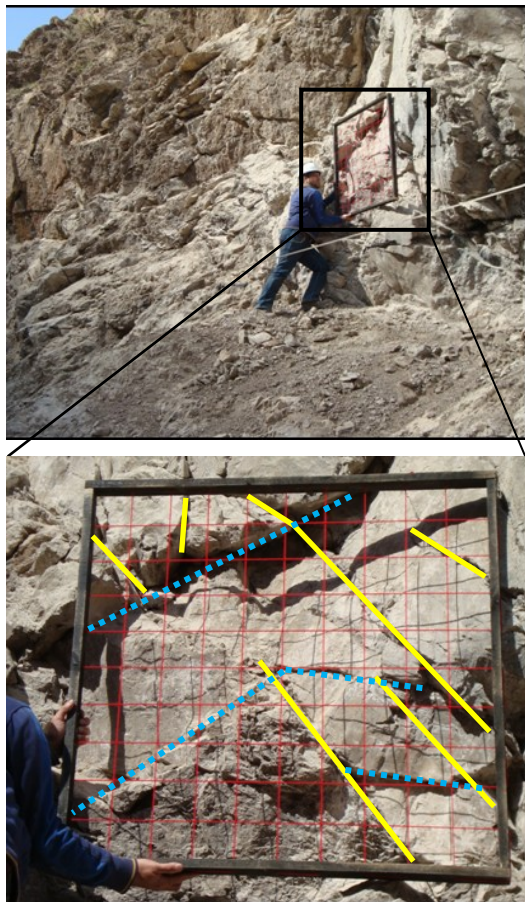


Figure 4. Joint intensity measurement, P21.

4.2.3. Spacing distribution

Based on the field measurements, spacing distribution of the discontinuities for different types of sedimentary, igneous, and metamorphic rocks can be modelled with negative exponential probability density distribution function [9, 32]. Furthermore, Priest [12] has proved that if the

fracture locations are random, the probability density distribution function of the fracture spacing would be negative exponential. Therefore, in this work, negative exponential distribution was used for spacing.

4.2.4. Persistence distribution

Fracture trace length, which is a result of the fracture coincidence with the exposure surface, indicates the expansion of fracture plane. Since direct surveying of the discontinuities inside the rock is impossible, there are a few studies regarding the 3D fracture surveying [34]. Therefore, practically, it is supposed that the 3D fracture measurements have statistical features similar to the results obtained from the 2D surveying [18]. Usually, for distribution of fracture trace length, three functions of negative exponential [9, 13, 35, 36], lognormal [12, 15, 37], and Gamma [12, 15] are used, which can be obtained from the 2D fracture surveying.

In this work, three Goodness of Fit (GOF) tests, the Kolmogorov-Smirnov test, the Anderson-Darling test, and the Chi-Squared test were used to evaluate the probability distribution of the rock fracture trace length. Regarding the previous investigations, the GOF test statistics were calculated for lognormal, Gamma, and exponential distribution functions separately. The results of the GOF test statistic values are shown in Figure 5. The features of fitted distribution functions of the fractures length in each fracture set are presented in Table 2.

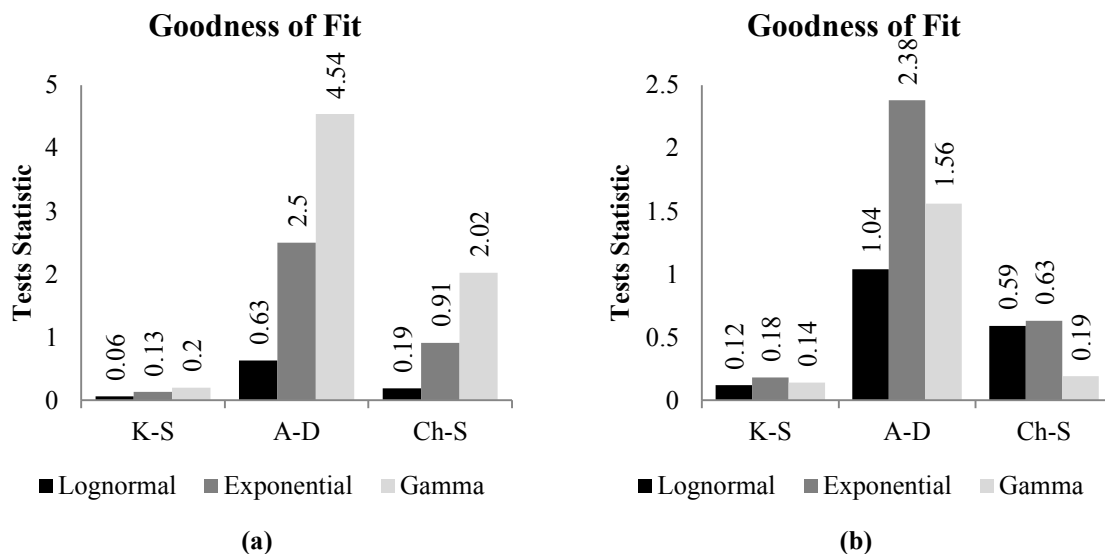


Figure 5. Comparison views of GOF test statistic values for (a) Joint set No. 1 (b) Joint set No. 2.

4.3. Model building

In stochastic modeling, the general approach is to treat locations, orientation, persistence (size), and other properties of the fractures as random variables with inferred probability distributions.

In order to model the fracture network, the fractures are grouped in fracture sets, which are identified from the statistics of the measured data and the geologic history of the region. The model building starts with generation of fracture set planes. Each set is modeled separately, and the final simulation is the simple combination of all independently simulated sets. In this method, fracture production inside the model continues until the number of fractures crossing the borehole or surveying surface is reproduced. The fracture intensity is controlled in the model through direct comparison of the observed and stimulated fractures. In this work, for stochastic fracture network modeling, a computer code written in C++ called DFN-FRAC^{3D} [6, 7] was used.

In the DFN-FRAC^{3D} program, a fracture set is characterized by the following five parameters:

- a) Fractures center location;
- b) Probability density function (PDF) of variation of fracture plane orientations including uniform, partial uniform, and Fisher;
- c) Mean orientation of fracture set;
- d) Fracture intensity;
- e) PDF of variation of fracture plane persistence including lognormal, Gamma, and exponential distribution functions.

In the current version of the DFN-FRAC^{3D} program, the fractures are convex polygonal planar objects of discontinuous rock, randomly oriented and located in 3D spaces. The presented model incorporates the Poisson plane and line stochastic processes. A fracture set is generated by

applying a sequence of four stochastic processes in space:

- First process: Create a homogeneous Poisson network of planes in space.
- Second process: Sub-divide each plane into a fractured region and its complementary region of intact rock by a homogeneous Poisson line network.
- Third process: Mark created polygons in previous step based on shape and size.
- Fourth process: Shift the polygons, which have been marked as fractured in the vicinity of their original position randomly.

It should be noticed that the fracture system including the fracture sets is generated by reiteration of the presented processes. The DFN-FRAC^{3D} program produces fracture sets with specific variations in shape and size based on some stochastic processes. Therefore, a more realistic representation of the natural rock fracture systems is provided. In this model, only polygons with shapes similar to the shapes of natural fractures remain. A polygon has a suitable shape, and is considered as a fracture if it has the following conditions: a) the polygon has at least four vertices; b) all angles are at least 60 degrees; c) the polygon elongation is not more than the permitted value. A polygon is retained with probability $P = 1.0$ if it has an appropriate shape, and discarded otherwise. More details related to the DFN-FRAC^{3D} program can be found in references [6] and [7].

In Figure 6, simulation of the stochastic discrete fracture networks of the diversion tunnel of Lorestan Rudbar dam is shown based on the geometrical parameters presented in Table 2 and the use of the DFN-FRAC^{3D} program. This simulated fracture network shows 15953 fractures in an area with $80 \times 80 \times 100$ cubic meters size.

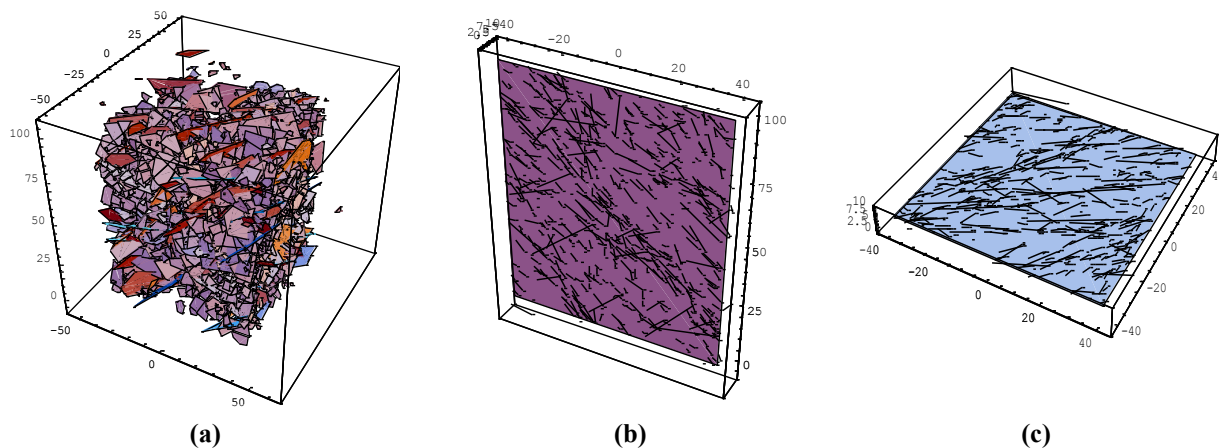


Figure 6. Simulated stochastic joint network of right wall of Rudbar Lorestan dam: a) 3D joint system; b) vertical trace outcrop; c) horizontal trace outcrop.

5. Tunnel stability and support analysis

The next step in the investigation of the mechanical behavior of underground structure is to analyze the stability of rock masses around an underground excavation. A reliable stability analysis and prediction of the support capacity are some of the most difficult tasks in rock engineering. In this section, first, the actual engineering geological conditions and the installed rock supports are described. Subsequently, the stability analyses are carried out for the tunnel by taking into account the stochastic fracture networks, rock mass parameters, and maximum expected ground water pressure after impoundment.

5.1. Estimation of rock mass properties

The rock mass geomechanical properties of the studied area were determined by laboratory testing on the intact rock samples. The rock mass properties such as Hoek–Brown constants, deformation modulus (E_{mass}), and uniaxial compressive strength (σ_{cmass}) were calculated by means of the RocLab software (Table 3) [38].

The values selected to represent fracture mechanical properties in the numerical model are

shown in Table 4. The friction angles of the discontinuities were estimated by taking into account their actual surface properties (degree of roughness (Jr) and weathering (Ja)) based on the approach suggested by Barton (2002). Regarding the joints and faults, a conservative estimation for friction angle ($\phi = 27^\circ$) with no cohesive strength was taken into account for the stability analysis [38]. Fractures were considered to be open and smooth with no filling material. Accordingly, cohesion was set to zero for the fractures [38].

5.2. Installed rock supports in tunnel

The planned and installed rock support measures accordingly in terms of different rock mass classification systems and based on the finite element method (without considering fractures) are included in the following items:

- 20 cm reinforced shotcrete in the area above spring line;
- 70 cm reinforced shotcrete in the area below spring line.

Characteristics of the support measures are shown in Table 5.

Table 3. Estimated geomechanical parameters for studied area [38].

Property	Value
Lithology	Broken dolomitic limestone
Material type	elasto-plastic
GSI (average)	30
Cohesion (MPa)	0.296
Friction angle (deg.)	36
Tensile strength (MPa)	0.014
UCS (MPa)	0.430
Modulus of deformation (MPa)	1581
Global strength (MPa)	2.60
Possion ratio	0.32
m_b constant	0.74
s constant	0.0004
a constant	0.522
Dilation parameter (deg.)	0
m_b constant (residual)	0.37
s constant (residual)	0.0002
Rock unit weight (kN/m^3)	27

Table 4. Mechanical property values of joints [38].

Property	Value
Friction angle (deg.)	27
Cohesion (MPa)	0

Table 5. Mechanical characteristics of support measures [38].

Property	Value
Young's modulus (GPa)	24
Poisson's ratio	0.2
Compressive strength (MPa)	24
Tensile strength (MPa)	2.4
Unit weight (kN/m^3)	24

5.3. Numerical analysis

In order to verify the installed support, a 2D hybrid element model, called Finite Element Program PHASE² Version 8.005 [39], was used in the numerical analysis conducted here in, since the program has been specially designed to handle a wide range of mining and civil engineering problems in a user friendly way. The Hoek–Brown failure criterion was used to identify elements undergoing yielding and the plastic zones of rock masses in the vicinity of tunnel perimeter. Plastic post-failure strength parameters were used in this analysis, and residual parameters were assumed as half of the peak strength parameters.

A horseshoe shaped tunnel with a 7 m span and 10 m height was excavated at a maximum depth of 100 m below surface. Vertical stress (σ_z) is a function of overburden. In situ stress for the finite element model was considered as hydrostatic. It is to be noted that for modeling the in-situ stresses, the actual ground elevation was considered in the model. The ground water head above the tunnel after impounding was around 37-60 m. In the stability analysis, the maximum water head of 60 m was considered, which is reasonably conservative. In the FEM analysis, the seismic load was considered by taking into account the horizontal and vertical values of 0.2 g and 0.08 g, respectively [38]. The vertical trace coordination of generated fractures using DFN model (Figure 6-b) were employed for numerical analysis. The properties of rock mass, fractures, and shotcrete lining assumed in this analysis were all obtained from the values given in Tables 3, 4, and 5, respectively. The outer model boundary was set at a distance of 3 times the tunnel radius.

For considering fractures and not considering fracture cases, the size of plastic zones, yielded elements, and maximum total displacements at wall, roof, and floor of the tunnel are shown in Figure 7. It should be remembered that PHASE² is a small strain finite element program, and thus it cannot accommodate the very large strains. Therefore, when Figure 7 is examined, it is more

important to consider the extent of plastic zone and yielded elements rather than the magnitude of the displacements.

In order to obtain tunnel stability, based on stability analysis assuming continuum media (without considering fractures), 200 mm thick reinforced shotcrete in the area above spring line and 700 mm thick reinforced shotcrete in the area below spring line were applied [38]. Acceptable maximum total displacements and yielded elements are shown in Figure 7-a. As it can be seen in Figure 7-b, after adding fractures into the model, the extent of plastic zone and yielded elements suggest that there would be a stability problem for tunnel. Therefore, the use of an additional support was found to be necessary for tunnel, so as to minimize the yielded elements and to reduce the size of total displacements. Consequently, 300 mm thick reinforced shotcrete in the area above spring line and 800 mm thick reinforced shotcrete in the area below spring line were used as support elements. After new support installation, not only the number of yielded elements but also the maximum total displacements decreased, as shown in Figure 7-c. This indicates that the applied support systems were adequate to obtain tunnel stability.

The number of yielded elements and maximum total displacements obtained from PHASE² FEM analysis with and without considering fracture cases are presented in Table 6.

For more explanation, the principle stresses and the strength factor distribution around tunnel, and also axial force, bending moment, and shear force in reinforced shotcrete are shown in Figure 8. As shown in this figure, after adding fractures into the model, the values of forces and moment in reinforced shotcrete increased. In the following, after new support installation, these values are reduced to some initial values.

The values of stresses around tunnel and minimum and maximum forces in reinforced shotcrete obtained by the PHASE² FEM analysis for with and without considering fracture cases are presented in Table 7.

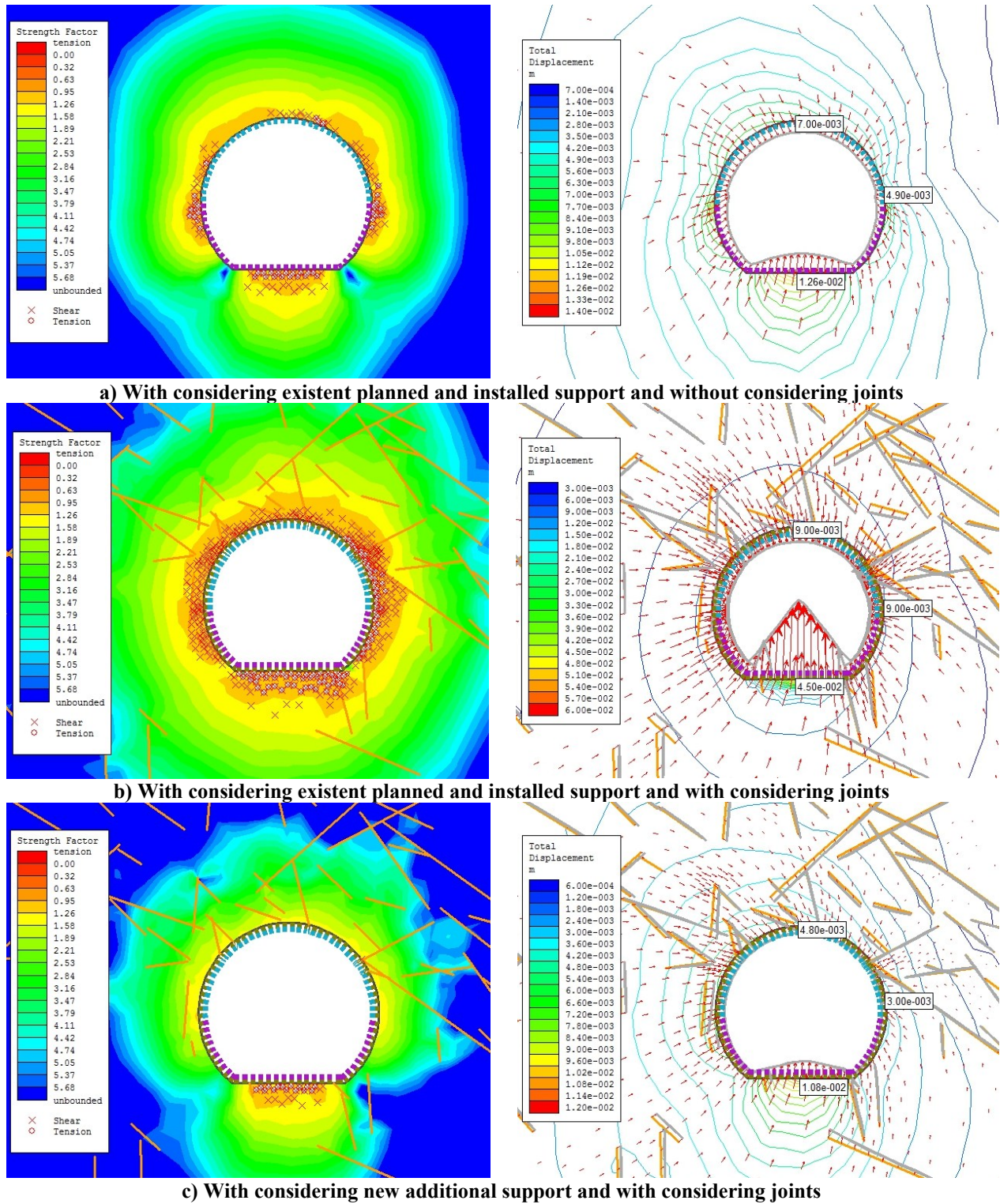


Figure 7. Displacement behavior (displayed dis. equal to 100 times actual dis.) and extent of plastic zone before and after adding joints.

Table 6. Number of yielded elements and maximum total displacements before and after considering joints.

Parameter	Location	Before considering joints	After considering joints	After installing additional 10 cm shotcrete
Total displacement (m)	Roof	7.00e-003	9.00e-003	4.80e-003
	Wall	4.90e-003	9.00e-003	3.00e-003
	Floor	1.26e-002	4.50e-002	1.08e-003
Number of yielded elements	---	106	343	25

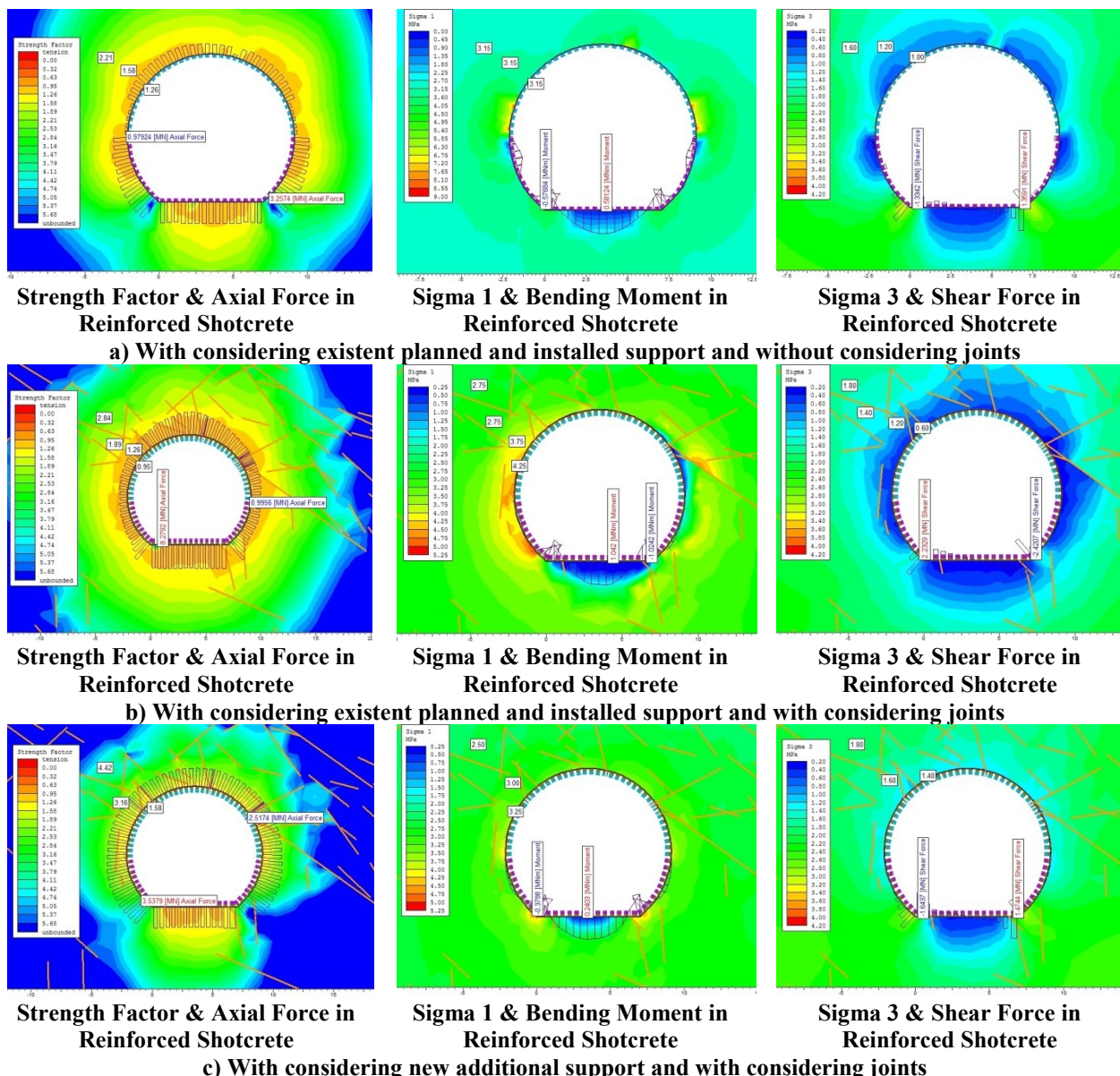


Figure 8. Principle stress distribution around tunnel and distribution of forces in reinforced shotcrete before and after adding joints.

Table 7. Values of stresses around tunnel and forces in reinforced shotcrete before and after considering joints.

Parameter	Before considering joints	After considering joints	After installing additional 10 cm shotcrete
Strength Factor	1.26	0.95	1.58
Sigma 1 (MPa)	3.15	4.25	3.25
Sigma 3 (MPa)	1.00	0.60	1.40
Axial Force (MN)	3.2574	8.2792	3.5379
Bending Moment (MN.m)	0.5812	1.042	0.2403
Shear Force (MN)	1.3591	2.2329	1.4744

6. Conclusions

In this work, the stability assessment and the design of the diversion tunnel constructed in the Rudbar Lorestan dam site (Iran) was investigated. The main goal was consideration of the 3D stochastic fracture network as the best choice for simulating the probability nature of fractured rock

mass in conjunction with a continuum stress analysis, which is capable of incorporating the finite size fracture explicitly in order to check the validity of the previous existent tunnel support systems in the mode of existing the effect of joints in stability analysis. For this purpose, 3D geometrical-stochastical model of joint network

around the selected diversion tunnel was prepared through the use of the DFN-FRAC^{3D} developed code. Using statistical studies on the geometrical features of the existing joint sets at the studied area, the required inputs for the computer code were provided. For numerical analysis, the finite element software PHASE² was used to determine the plastic zones and deformations developed around the rock mass surrounding the tunnel. As well as the principle stresses and the strength factor distribution around tunnel, axial force, bending moment, and shear force in reinforced shotcrete were specified. According to the results obtained, there were some stability problems for tunnel by considering the effect of joints. For the selected tunnel, coverage of old tunnel support units with an about 10 cm shotcrete application was determined to be sufficient, providing a long term stability. After considering these additional support elements, the numerical analysis showed that there was a considerable decrease in both the number of yielded elements and the size of total displacements around the tunnel.

References

- [1]. Bieniawski, Z.T. (1973). Engineering classification of jointed rock masses. *Trans South Afr Inst Civ Eng.* 15: 335-44.
- [2]. Long, J.C.S. and Witherspoon, P.A. (1985). The relationship of the degree of interconnection and permeability in a fracture network. *Journal of Geophysics Research.* 90: 3087-3097.
- [3]. Pine, R.J., Coggan, J.S., Flynn, Z. and Elmo, D. (2006). The development of a comprehensive numerical modeling approach for pre-fractured rock masses. *Rock Mechanics and Rock Engineering.* 39 (5): 395-419.
- [4]. Park, H.J. and West, T.R. (2001). Development of a probabilistic approach for rock wedge failure. *Engineering Geology.* 59: 223-251.
- [5]. Wu, Q. and Kulatilake, P.H.S.W. (2012). Application of equivalent continuum and discontinuum stress analyses in three-dimensions to investigate stability of a rock tunnel in a dam site in China. *Computers and Geotechnics.* 46: 48-68.
- [6]. Noroozi, M., Kakaie, R. and Jalali, S.E. (2015). 3D Geometrical-Stochastic Modeling of Rock mass Joint Networks (Case Study: the Right Bank of Rudbar Lorestan Dam Plant). *Journal of Geology and Mining Research.* 7 (1): 1-10.
- [7]. Noroozi, M., Kakaie, R. and Jalali, S.E. (2015). 3D stochastic rock fracture modeling related to strike-slip faults. *Journal of Mining & Environment.* 6 (2): 169-181.
- [8]. Noroozi, M., Kakaie, R. and Jalali, S.E. (2014). Review of Synthetic Rock Mass Model for Determining the Strength Characterization of Rock. 32nd National & the 1st International Geosciences Congress. Iran (In Persian).
- [9]. Baecher, G.B. (1983). Statistical analysis of rock mass fracturing. *Journal of Mathematical Geology.* 15 (2): 329-347.
- [10]. Einstein, H.H., Veneziano, D., Baecher, G.B. and O'Reilly, K.J. (1983). The effect of discontinuity persistence on rock slope stability. *International journal of rock mechanics and mining sciences & geomechanics abstracts.* 20 (5): 227-236.
- [11]. Dershowitz, W.S. and Einstein, H.H. (1988). Characterizing rock joint geometry with joint system models. *Rock Mechanics and Rock Engineering.* 21: 21-51.
- [12]. Priest, S.D. (1993). *Discontinuity Analysis for Rock Engineering.* Published by Chapman & Hall. London.
- [13]. Kulatilake, P.H.S.W. (1993). Application of probability and statistics in joint network modeling in three dimensions. *Proceedings of the conference on probabilistic methods in geotechnical engineering.* Canberra. Australia pp. 63-87.
- [14]. Ivanova, V., Yu, X., Veneziano, D. and Einstein, H. (1995). Development of stochastic models for fracture systems. In *The 35th US Symposium on Rock Mechanics (USRMS).* American Rock Mechanics Association.
- [15]. Zhang, L. and Einstein, H.H. (2000). Estimating the Intensity of Rock Discontinuities, *International Journal of Rock Mechanics and Mining Science,* 37: 819-837.
- [16]. Kulatilake, P.H.S.W., Park, J. and Um, J. (2004). Estimation of rock mass strength and deformability In 3-D for a 30 m cube at a depth of 485 m at Aspo Hard Rock Laboratory. *Geotechnical and Geological Engineering.* 22: 313-330.
- [17]. Baghbanan, A. and Jing, L. (2008). Hydraulic properties of fractured rock masses with correlated fracture length and aperture. *International Journal of Rock Mechanics & Mining Sciences.* 44: 704-719.
- [18]. Xu, C. and Dowd, P. (2010). A new computer code for discrete fracture network modeling. *Computers & Geosciences.* 36: 292-301.
- [19]. Bang, S.H., Jeon, S.W. and Kwon, S.K. (2012). Modeling the hydraulic characteristics of a fractured rock mass with correlated fracture length and aperture: application in the underground research tunnel at Kaeri. *Nuclear engineering and technology.* 44(6): 639-652.
- [20]. Yoshida, H. and Horii, H. (2004). Micromechanics-based continuum model for a jointed

rock mass and excavation analyses of a large-scale cavern. *Int. J. Rock Mech. Min. Sci.* 41: 119-145.

[21]. Sitharam, T.G., Sridevi, J. and Shimizu, N. (2001). Practical equivalent continuum characterization of jointed rock masses. *Int. J. Rock Mech. Min. Sci.* 38: 437-448.

[22]. Sitharam, E.G. and Latha, G.M. (2002). Simulation of excavations in jointed rock masses using a practical equivalent continuum approach. *Int. J. Rock Mech. Min. Sci.* 39: 517-525.

[23]. Torano, J., Rodriguez, R., Rivas, J.M. and Casal, M.D. (2002). FEM modeling of roadways driven in a fractured rock mass under longwall influence. *Comput Geotech.* 29: 411-431.

[24]. Zhu, W., Shuca, L., Shuchen, L., Chen, W. and Lee, C.F. (2003). Systematic numerical simulation of rock tunnel stability considering different rock conditions and construction effects. *Tunnelling and Underground Space Technology.* 18: 531-536.

[25]. Basarir, H. (2006). Engineering geological studies and tunnel support design at sulakyurt dam site, Turkey. *Engineering Geology.* 86: 225-237.

[26]. Genis, M., Basarir, H., Ozarslan, A., Bilir, E. and Balaban, E. (2007). Engineering geological appraisal of the rock masses and preliminary support design, Dorukhan tunnel, Zonguldak, Turkey. *Engineering Geology.* 92: 14-26.

[27]. Cai, M. (2008). Influence of stress path on tunnel excavation response- numerical tool selection and modeling strategy. *Tunnelling and Underground Space Technology.* 23: 618-628.

[28]. Coggan, J., Gao, F., Stead, D. and Elmo, D. (2012). Numerical modeling of the effects of weak immediate roof lithology on coal mine roadway stability. *International Journal of Coal Geology.* 90-91: 100-109.

[29]. Secondly Engineering Geology Report. (2007). Rudbar Lorestan Dam & Hydropower Plant. Iran Water & Power Resources development Co.

[30]. Weiss, M. (2008). Techniques for estimating fracture size: A comparison of methods. *International*

Journal of Rock Mechanics & Mining Sciences. 15: 460-466.

[31]. Kulatilake, P.H.S.W., Chen, J., Teng, J., Shufang, X. and Pan, G. (1996). Discontinuity Geometry Characterization in a Tunnel Close to the Proposed Permanent Shiplock Area of the Three Gorges Dam site in China. *International Journal of Rock Mechanics, Mining Science & Geomechanics Abstract.* 33 (3): 255-277.

[32]. Noroozi, M., Jalali, S.E. and Kakaei, R. (2013). Statistical relationship on discontinuities geometrical properties, International Conference on Mining Mineral Processing, Metallurgical and Environmental Engineering. Zanjan, Iran. (In Persian).

[33]. Lin, A. and Yamashita, K. (2013). Spatial variations in damage zone width along strike-slip faults: An example from active faults in southwest Japan. *Journal of Structural Geology.* 57: 1-15.

[34]. Dowd, P.A., Xu, C., Mardia, K.V. and Fowell, R.J. (2007). A comparison of methods for the simulation of rock fractures. *Mathematical Geology.* 39: 697-714.

[35]. Kulatilake, P.H.S.W., Um, J., Wang, M., Escandon, R.F. and Varvaiz, J. (2003). Stochastic fracture geometry modeling in 3-D including validations for a part of Arrowhead East Tunnel, California, USA. *Eng Geol.* 70: 131-155.

[36]. Zadhesh, J., Jalali, S.M.E. and Ramezanzadeh, A. (2014). Estimation of joint trace length probability distribution function in igneous, sedimentary, and metamorphic rocks. *Arabian Journal of Geosciences.* 7 (6): 2353-2361.

[37]. Wu, F. and Wang, S. (2002). Statistical model for structure of jointed rock mass. *Geotechnique.* 52 (2): 137-140.

[38]. New Diversion Tunnel Report. (2013). Rudbar Lorestan Dam & Hydropower Plant. Iran Water & Power Resources development Co.

[39]. Rocscience (2011). PHASE² Version 8.005. User's Guide, Rocscience Inc. 31 Balsam Ave., Toronto, Ontario M4E 1B2, Canada.

تحلیل پایداری سیستم‌های نگهداری با استفاده از روش توأمان FEM-DFN (مورد مطالعاتی: تونل انحراف سد رودبار لرستان، ایران)

مهدی نوروزی^{۱*}، رامین رفیعی^۱ و مهدی نجفی^۲

۱- دانشکده مهندسی معدن، نفت و ژئوفیزیک، دانشگاه صنعتی شاهرود، ایران

۲- دانشکده مهندسی معدن و متالورژی، دانشگاه یزد، ایران

ارسال ۲۰۱۷/۷/۲۸، پذیرش ۲۰۱۸/۲/۱۴

* نویسنده مسئول مکاتبات: mehdi.noroozi@shahroodut.ac.ir

چکیده:

ناپیوستگی‌های ساختاری مختلف که شبکه ناپیوستگی‌های مجزا را تشکیل می‌دهند، نقش مهمی در شرایط شکست و پایداری توده‌های سنگی اطراف حفاری‌های زیرزمینی بازی می‌کنند. تاکنون چندین روش عددی پیوسته برای مطالعه پایداری حفاری‌های زیرزمینی در توده سنگ‌های درزه‌دار به کار برده شده است، اما فقط تعداد کمی از آن‌ها تأثیر ناپیوستگی‌های طبیعی از قبل موجود را در نظر گرفته‌اند. در این مطالعه، ناپیوستگی‌های از قبل موجود به طور دقیق به صورت مدل شبکه ناپیوستگی‌های مجزا (DFN) مدل‌سازی می‌شوند. سپس این مدل با مدل FEM برای تحلیل پایداری سیستم‌های نگهداری تونل انحراف سد رودبار لرستان تلفیق می‌شود. برای این منظور، در ابتدا، با استفاده از اطلاعات برداشت شده در تونل انحراف و تخمین توابع چگالی احتمال مناسب برای ویژگی‌های هندسی دسته درزه‌های موجود در این منطقه، مدل DFN سه‌بعدی با استفاده از برنامه مولد شبکه ناپیوستگی‌های مجزای تصادفی، DFN-FRAC^{3D}، شبیه‌سازی شد. در مرحله دوم، تلفیق روش المان محدود دوبعدی و مدل تصادفی تهیه شده برای تحلیل سیستم‌های نگهداری پیشنهاد شده موجود (بر اساس گزارش‌های فنی) به کار برده شده است. هدف در اینجا فهم نقش شبکه ناپیوستگی‌ها بر نتایج تحلیل پایداری تونل، زمانی که از مدل‌سازی FEM استفاده می‌شود و همچنین مقایسه نتایج تحلیل پایداری در دو حالت با در نظر گرفتن اثر ناپیوستگی‌ها و بدون در نظر گرفتن اثر ناپیوستگی‌ها است.

کلمات کلیدی: تحلیل پایداری تونل، روش المان محدود، شبکه درزه‌های مجزا.